Planar Voronoi cells and the failure of Aboav's law

Hendrik-Jan Hilhorst

Planar Voronoi cells and the failure of Aboav's law

H.J. Hilhorst*
Laboratoire de Physique Théorique, Bâtiment 210, Université de Paris-Sud, 91405 Orsay, France
(Dated: September 15, 2005)

Aboav's law is a quantitative expression of the empirical fact that in planar cellular structures many-sided cells tend to have few-sided neighbors. This law is nonetheless violated in the most widely used model system, *viz.* the Poisson-Voronoi tessellation. We obtain the correct law for this model: Given an n-sided cell, any of its neighbors has on average m_n sides where $m_n = 4 + 3(\pi/n)^{-\frac{1}{2}} + \ldots$ in the limit of large n. This expression is quite accurate also for nonasymptotic n and we discuss its implications for the analysis of experimental data.

Two empirical rules play a key role in studies of planar cellular systems: Lewis' law and Aboav's law. Both are statements about the statistics of a cell's most prominent properties, *viz.* its area and its number of sides. Lewis' law [1] says that the average area A_n of an n-sided cell increases with n as $A_n = a_0(n - n_0)/\lambda$, where a_0 and n_0 are constants, and λ is the two-dimensional cell density. Aboav [2] noticed that many-sided cells tend to have few-sided neighbors and *vice versa.* He expressed this correlation in terms of the average m_n of the number of sides of a cell that neighbors an n-sided cell. Aboav's law, also called the Aboav-Weaire [3] law, asserts that

$$m_n = a + \frac{b}{n}\,, \tag{1}$$

where a and b are constants. This law is in widespread use [4, 5, 6, 7, 8, 9, 11, 12, 13, 14, 15] in the analysis of experimental data on cellular structures.

In nature, planar cellular systems come in a wide variety. They include biological tissues [1, 4, 5], polycrystals [2], cells formed by particles trapped at a water/air interface [6], cells in surface-tension driven Bénard convection [7], in two-dimensional soap froths [8], and in magnetic liquid froths [9].

Alternatively, the cellular structure may appear when the data are subjected to the Voronoi construction [10]. Examples are hard disks on an air table [11], a binary liquid during late stage coarsening [12], two-dimensional colloidal aggregation [13], nanostructured cellular layers [14], and studies of two-dimensional melting [15].

Many of these cellular systems, in spite of all their diversity, closely obey Lewis' law from $n \approx 5$ up; also in many, Aboav's law appears to hold with good accuracy in the full experimentally accessible range, *i.e.* from $n = 3$ to n typically between 9 and 12. Fitting (1) to experimental data leads to values for the coefficient a ranging from 4.6 to 5.3 and for b from 7.0 to 8.5. This observed similarity of behavior, sometimes called "universality," is generally attributed to the strong geometrical constraints that accompany a division of the plane into convex cells; by contrast, physical or biological mechanisms are believed only to lead to corrections. It is of obvious interest to subtract from the experimental data any purely geometrical effect that one can isolate in order to identify the mechanisms at work that cause the corrections.

Although Lewis' and Aboav's laws arose initially merely as good descriptions of the available data, several "derivations" have since conferred to them the status of theoretical truths valid for all n and embodying a purely geometrical theory. Most attempts [16] to derive these laws apply maximum entropy principles to a hypothesized entropy functional [17]. A critique of this usage of the maximum entropy method is due to Chiu [18], who has shown that no firm conclusions can be drawn from it. In any case, none of these derivations connects either Lewis' or Aboav's law by a first principle calculation to a microscopic model of planar cellular structure.

First-principle approach. – The simplest microscopic model of a planar cell model is the Poisson-Voronoi (PV) tessellation: It is obtained by constructing the Voronoi cells [10] of a configuration of randomly and uniformly distributed *point centers* in the plane, for convenience often called "seeds" (but without the implication that they are material). The PV tessellation is therefore a natural candidate for the purely geometrical theory, and certainly the easiest one to handle.

The statistical properties of the PV tessellation have been studied analytically and by Monte Carlo methods (see Ref. [10] for a review). Nonetheless, a first principle derivation of expressions for A_n and m_n has long seemed forbiddingly difficult. Numerically it is known [19, 20, 21, 22] that Aboav's law is *not* exactly valid for the Poisson-Voronoi tessellation: Whereas Eq. (1) predicts nm_n to be linear in n, this quantity shows in fact a very small but distinct downward curvature for the PV tessellation. To accommodate this discrepancy modifications of Aboav's law have been suggested, in particular, by Boots and Murdoch [19] and by LeCaër and Ho [20]. The former authors write $m_n = A + Bn^{-1} + Cn^{-2}$, which was later found to be true exactly for a class of graphs in field theory [23].

A recent letter [24] has achieved a step forward in the statistical mechanics of planar Voronoi tessellations. It opens up the possibility for an expansion in powers of $n^{-\frac{1}{2}}$ of all quantities of interest related to the n-sided Voronoi cell; an immediate result was that Lewis' law holds with coefficient $a_0 = \frac{1}{4}$ for asymptotically large n.

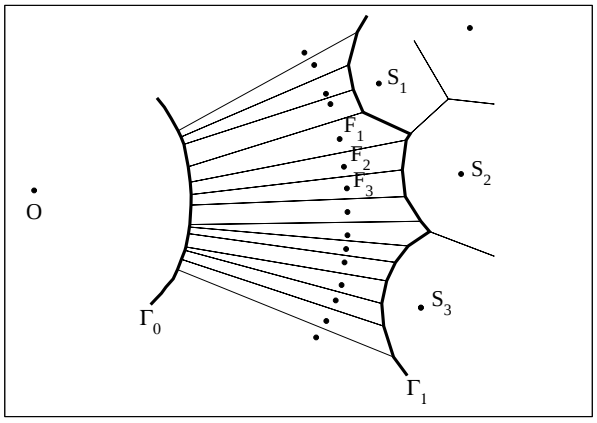

FIG. 1: Schematic picture of an n-sided Voronoi cell having $n \approx 100$ and containing a seed at O. First and second neighbor cells contain seeds at $F_1, F_2, F_3, \ldots$ and at $S_1, S_2, S_3, \ldots$, respectively. All solid line segments separate Voronoi cells. Among these, the heavy solid line Γ_0 is the perimeter of the n-sided cell, which is close to circular. The heavy solid line Γ_1 separates the first from the second neighbors. Both are piecewise linear on a scale $n^{-\frac{1}{2}}$. On the scale of order 1 the incipient piecewise parabolic structure of Γ_1 is discernible.

Aboav's law. – Whereas Lewis' law refers to a single cell, Aboav's deals with the intrinsically more difficult problem of correlations between cells. Here we track down the implications of the $n^{-\frac{1}{2}}$ expansion for Aboav's law. We consider an n-sided cell with n very large. Cells with very many sides are extremely rare, but *if* one occurs, then its environment must look as depicted in Fig. 1, where the n-sided cell of a "central" seed at O is surrounded by n strongly elongated first neighbor cells containing seeds F_i. Independent evidence for such a geometry comes from work by Lauritsen *et al.* [22], who Monte Carlo simulated a Hamiltonian favoring the appearance of many-sided cells.

In Fig. 1 at least four different length scales play a role, each of them proportional to its own power of n. Heavily relying on the work of Ref. [24], which for the present purpose we extend and interpret, we establish the following list of scales:

(i) The perimeter Γ_0 of the central cell typically runs within an annulus of center O, of radius $R_c = (n/4\pi\lambda)^{\frac{1}{2}}$, and of width of order 1. Hence for $n \to \infty$ the perimeter tends towards a circle of radius R_c. Consequently in that limit the first neighbors F_i will be on a circle of radius $2R_c$.

(ii) Two successive vertices on the perimeter of the central cell have an average distance $\ell_{\rm vert} = 2\pi R_c/n = (\pi/n\lambda)^{\frac{1}{2}}$. Consequently, two successive first neighbor seeds F_i and F_{i+1} have an average distance $2\ell_{\rm vert}$.

(iii) Locally the positions of the vertices of the central cell are strongly aligned: Their radial coordinates have rms deviations of order $n^{-\frac{3}{2}}$ with respect to the locally averaged radius. For the purpose of the present discussion we may set these deviations equal to zero; their smallness implies that for $n \to \infty$ the perimeter of the central cell becomes a smooth curve. Similar statements hold for the curve, not drawn in the Fig. 1, that links the successive first neighbors.

(iv) In the region to the right of the heavy solid line Γ_1, which is occupied by second and further neighbors, the seed density has its "background" value λ, *i.e.* is of order n^0 [25].

On the basis of this picture we reason as follows. The perimeter of the central cell carries a vertex line density $\rho_{\rm vert} = 1/\ell_{\rm vert} = (n\lambda/\pi)^{\frac{1}{2}}$, which for $n \to \infty$ tends to infinity. In spite of this diverging line density the surface density λ of the seeds to the right of the curve Γ_1 stays of order n^0. It follows that the central cell will have $\sim n^{\frac{1}{2}}$ second neighbor cells and that each second neighbor S_j will be adjacent to $\sim n^{\frac{1}{2}}$ first neighbor cells F_i (where we call the cells by the names of their seeds). Fig. 1 shows that under these circumstances each first neighbor F_i is most likely to have itself four neighbors, *viz.* the central n-sided cell, a single second neighbor cell, and two other first neighbors, F_{i-1} and F_{i+1}.

We now focus on the exceptional F_i that have five neighbors due to their being adjacent to *two* second neighbors S_j and S_{j+1}. An example is the cell marked F_1 in Fig. 1, which is adjacent to both S_1 and S_2. Let us denote by f_5 the fraction of first neighbors that are 5-sided. In view of the scaling relations that precede we expect that $f_5 = cn^{-\frac{1}{2}} + \ldots$, where c is a numerical coefficient and the dots indicate terms of higher order in $n^{-\frac{1}{2}}$. Any 6- and higher-sided F_i will contribute only to these dot terms. Hence we have

$$\begin{aligned} m_n &= 4\,(1 - f_5) + 5 f_5 \\ &= 4 + cn^{-\frac{1}{2}} + \ldots . \end{aligned} \tag{2}$$

We next consider the solid line Γ_1 in Fig. 1, which separates the central seed's first from its second neighbors. In the large n limit the curve linking successive first neighbor seeds becomes a circle which may locally be replaced with a straight line. In Fig. 2 this same straight line is represented by the x axis and the region of space containing the second and further neighbors by the half-plane $y > 0$. The second and further neighbor seeds are uniformly distributed in the upper half plane with the background density λ. Since the first neighbors F_i are dense on the x axis, the curve Γ_1 now divides the half-plane $y > 0$ into a lower part of points closer to the x axis than to any of the seeds, and its complement. Hence the function $y = \Gamma_1(x)$ is piecewise parabolic; its incipient parabolic segments are discernable in Fig. 1. To each cusp of $\Gamma_1(x)$ corresponds a 5-sided first neighbor cell. Let $\ell_{\rm cusp}$ be the average distance between the abscissae

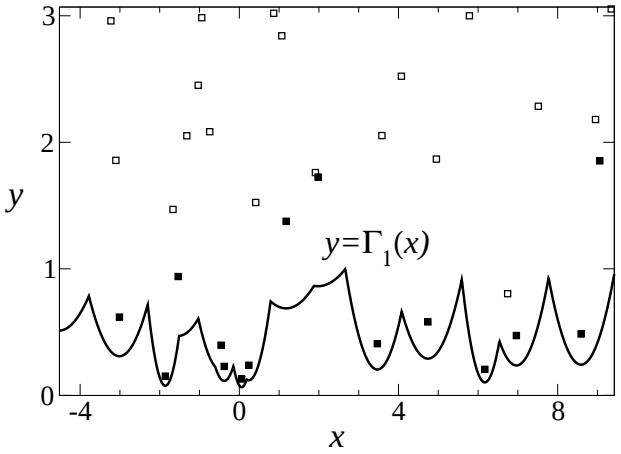

FIG. 2: The x-axis represents a continuum of first neighbors. The upper half-plane is randomly filled with seeds of uniform density λ (here $\lambda = 1$). The piecewise parabolic curve $y = \Gamma_1(x)$ separates the region of the half-plane closer to the x axis than to any of the random seeds from its complement. The abscissae of the cusps of Γ_1 have a density of $\frac{3}{2}\lambda^{\frac{1}{2}}$ on the x axis. Solid and open squares represent second and further neighbors, respectively. Note that the horizontal and vertical scales are different.

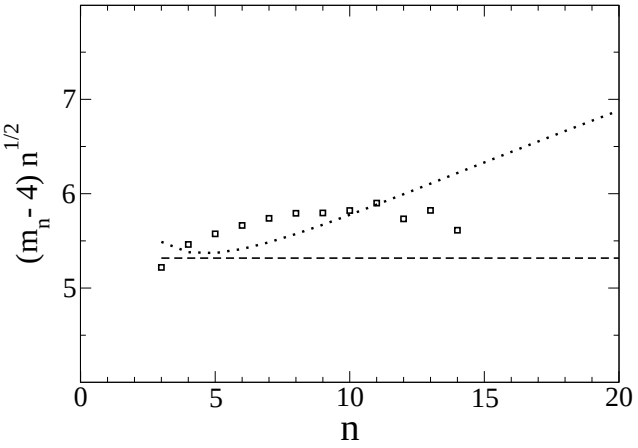

FIG. 3: The two-cell correlation m_n as a function of n. Open squares: Simulation values due to Boots and Murdoch [19]. Dotted line: Best two-parameter fit with Aboav's law (1). Dashed line: Our zero-parameter exact asymptotic result (3), which in this representation is a constant equal to $3\pi^{\frac{1}{2}}$.

of two successive cusps of $\Gamma_1(x)$. Then it is clear that $f_5 = 2\ell_{\rm vert}/\ell_{\rm cusp}$. The determination of $\ell_{\rm cusp}$ for given seed density λ in the upper half plane is a problem in statistics that yields $\ell_{\rm cusp} = 2/(3\lambda^{\frac{1}{2}})$ [26]. Using the expression for $\ell_{\rm vert}$ found above we therefore have that $f_5 = 2(\pi/n\lambda)^{\frac{1}{2}} \times 3\lambda^{\frac{1}{2}}/2 = 3(\pi/n)^{\frac{1}{2}}$, whence $c = 3\pi^{\frac{1}{2}}$. Substituting this in (2) we conclude that for the Poisson-Voronoi tessellation m_n is exactly given by

$$m_n = 4 + 3\sqrt{\frac{\pi}{n}} + \ldots, \qquad n \to \infty. \tag{3}$$

The inverse square root decay and the limiting value $m_\infty = 4$ of Eq. (3) are in contradistinction to Aboav's law (1). This equation explains for the first time the downward curvature observed [19, 20, 21, 22] in the nm_n *vs.* n curves for the PV tessellation.

Data analysis. – We cannot assess *a priori* the applicability of Eq. (3) to m_n data in the range of n covered by experiments and simulations. We have plotted in a new way in Fig. 3 the Monte Carlo data for m_n due to Boots and Murdoch [19]. The dotted curve shows the best two-parameter fit to the data provided by Aboav's law (1); it is obtained for $a = 5.251$ and $b = 5.755$ [10] and is generally taken as evidence that this law fails for the PV tessellation. The dashed line in Fig. 3 represents the right hand side of Eq. (3) with the dot terms neglected. It appears that in the regime of the data our zero-parameter asymptotic result is numerically only slightly more off than Aboav's two-parameter law [27]. This high degree of accuracy is remarkable in view of the fact that Eq. (3) rests on an expansion around the improbable event of a large n-sided cell. But more importantly, there is full compatibility between our dashed line and the downward trend of the data for n larger than about 10. One may attempt to improve our Eq. (3) by including higher order terms in $n^{-\frac{1}{2}}$ in the series, the simplest possibility being

$$m_n = 4 + 3\sqrt{\frac{\pi}{n}} + \frac{d}{n}, \tag{4}$$

where d is adjustable. However, there is no reason to expect that a truncated expression, whether (4), (1), or yet another one, will yield the exact m_n for all n.

The PV tessellation serves as a model of reference for general cellular systems much in the same way as an ideal gas does for real gases. The inverse square root decay of its two-cell correlation rules out Aboav's law (1) and may be viewed as defining a universality class. We cannot exclude that someday some other microscopic model will be shown to asymptotically obey Aboav's law (1) to leading order in n^{-1}. Such a model would then define a second universality class. It is unknown at present which experimental systems are in the PV universality class.

Many different factors may potentially lead to departures from PV-like behavior, if not to a change of universality class. *E.g.,* (i) in some cellular structures the "seeds" represent actual particles or larger physical entities with mutual interactions; (ii) a general planar cell structure cannot be derived from a set of point centers by means of the Voronoi construction; and (iii) some systems, like soap froths, are not in equilibrium but rather in a – supposedly scale invariant – coarsening state. One may now hope for such cases to be able to discuss the deviations from PV tessellation statistics perturbatively.

To show how such a discussion might proceed, we consider briefly and heuristically an example from class (ii) above, *viz.* the Voronoi tessellations associated with hard core particles of finite diameter a. The preceding analysis of the large n limit goes through as long as $n \lesssim n^*$, where the crossover value n^* is determined by the condition that the distance between adjacent first neighbors become comparable to the particle diameter. This gives $2\pi R_c \sim n^* a$, whence $n^* \sim \pi/(\lambda a^2)$. For $n \gtrsim n^*$ the repulsion between the particles combined with the condition that they be locally aligned imposes that the radius of the central cell grows as $R_c \sim na$ and hence that f_5 must saturate at a value $f_5 = c_0 a \lambda^{\frac{1}{2}}$ where c_0 is an unknown numerical coefficient. Upon assuming that this knowledge may be expressed with the aid of a scaling function $\mathcal{M}$ we obtain for hard core particles of diameter a the relation $m_n = 4 + a\lambda^{\frac{1}{2}}\mathcal{M}(n\lambda a^2)$, valid in the scaling limit $n \to \infty$, $\lambda a^2 \to 0$ with $x = n\lambda a^2$ fixed, and where the scaling function $\mathcal{M}$ satisfies $\mathcal{M}(0) = c_0$ and $\mathcal{M}(x) \simeq 3(\pi/x)^{\frac{1}{2}}$ for $x \to \infty$. Hence for hard core particles the limiting value m_∞ of (3) is changed, *but the* $n^{-\frac{1}{2}}$ *decay law remains.* Future work will have to deal with this and other instances of deviations from PV statistics.

Conclusion. – The simplest and most widely used model of a cellular structure – the Poisson-Voronoi tessellation – does not obey the most widely used law – Aboav's law (1) – governing the two-cell correlations. We have shown that for the PV tessellation the n^{-1} decay of Aboav's law should in fact be replaced with an $n^{-\frac{1}{2}}$ decay. Experimental data of sufficient precision and/or covering a large enough range should be able to distinguish between the two and thereby shed light on the question of the universality classes and of the underlying cell formation mechanisms. We therefore advocate that experimental results be analyzed not only by Aboav's two-parameter fit (1), but also by the simpler one-parameter formula (4), of which the first two terms have a firm theoretical basis.

Acknowledgment. – This work was made possible by a six month sabbatical period (CRCT) granted to the author by the French Ministry of Education.

* Electronic address: Henk.Hilhorst@th.u-psud.fr

[1] F. T. Lewis, *Anatomical Records* **38**, 341 (1928); **47**, 59 (1930); **50**, 235 (1931).
[2] D.A. Aboav, *Metallography* **3**, 383 (1970).
[3] D. Weaire, *Metallography* **7**, 157 (1974).
[4] J.C.M. Mombach, R.M.C. de Almeida, and J.R. Iglesias, *Phys. Rev. E* **47**, 3712 (1993).
[5] B. Jeune and D. Barabé, *Annals of Botany* **82**, 577 (1998).
[6] S.J. Mejía-Rosales, R. Gámez-Corrales, B.I. Ivlev, and J. Ruiz-García, *Physica A* **276**, 30 (2000).
[7] P. Cerisier, S. Rahal, and N. Rivier, *Phys. Rev. E* **54**, 5086 (1996).
[8] J.A. Glazier, S.P. Gross, and J. Stavans *Phys. Rev. A* **36**, 306 (1987); J. Stavans and J.A. Glazier, *Phys. Rev. Lett.* **62**, 1318 (1989).
[9] F. Elias, C. Flament, J.-C. Bacri, O. Cardoso, and F. Graner, *Phys. Rev. E* **56**, 3310 (1997).
[10] A. Okabe, B. Boots, K. Sugihara, and S. N. Chiu, *Spatial tessellations: concepts and applications of Voronoi diagrams,* second edition (John Wiley & Sons Ltd., Cichester, 2000).
[11] J. Lemaître, A. Gervois, J.P. Troadec, N. Rivier, M. Ammi, L. Oger, and D. Bideau, *Phil. Mag. B* **67**, 347 (1993).
[12] M. Seul, N.Y. Morgan, and C. Sire, *Phys. Rev. Lett.* **73**, 2284 (1994).
[13] J.C. Earnshaw and D.J. Robinson, *Phys. Rev. Lett.* **72**, 3682 (1994); *Physica A* **214**, 23 (1995).
[14] P. Moriarty, M.D.R. Taylor, and M. Brust, *Phys. Rev. Lett.* **89**, 248303 (2002).
[15] K. Zahn, R. Lenke, and G. Maret, *Phys. Rev. Lett.* **82**, 2721 (1999); R.A. Quinn and J. Goree, *Phys. Rev. E* **64**, 051404 (2001).
[16] N. Rivier and A. Lissowski, *J. Phys. A* **15**, L143 (1982); N. Rivier, *Phil. Mag. B* **52**, 795 (1985). M.A. Peshkin, K.J. Strandburg, and N. Rivier, *Phys. Rev. Lett.* **67**, 1803 (1991); C. Sire et M. Seul, *J. Phys. I France* **5**, 97 (1995); B. Dubertret, N. Rivier, and M.A. Peshkin, *J. Phys. A* **31**, 879 (1998).
[17] Alternative derivations rest on closure approximations for local averages, *e.g.* S.F. Edwards and K.D. Pithia, *Physica A* **205**, 577 (1994); Gy. Vincze, I. Zsoldos, and A. Szasz, *J. Geometry and Physics* **51**, 1 (2004).
[18] S. N. Chiu, *J. Phys. A* **28**, 607 (1995); *Materials Characterization* **34**, 149 (1995).
[19] B.N. Boots and D.J. Murdoch, *Computers and Geosciences* **9**, 351 (1983).
[20] G. Le Caër and J. S. Ho, *J. Phys. A* **23**, 3297 (1990).
[21] S. Kumar and S.K. Kurtz, *Materials Characterization* **31**, 55 (1993).
[22] K.B. Lauritsen, C. Moukarzel, and H.J. Herrmann, *J. Phys. I France* **3**, 1941 (1993).
[23] C. Godrèche, I. Kostov, and I. Yekutieli, *Phys. Rev. Lett.* **69**, 2674 (1992).
[24] H.J. Hilhorst, *J. Stat. Mech.* L02003 (2005); see also H.J. Hilhorst, *J. Stat. Mech.* P09005 (2005).
[25] Fig. 1 is schematic in that a faithful representation of all proportions would lead to an about twice higher density of the second and further neighbors to the right of Γ_1; as it is, the picture better brings out the emergence of the piecewise parabolic segments of Γ_1.
[26] H.J. Hilhorst, unpublished.
[27] A best fit of Eq. (2) without its dot terms to the Monte Carlo data yields a coefficient $c \approx 5.7$, only slightly higher than the exact value $c = 3\pi^{\frac{1}{2}} = 5.317\ldots$.